Effect of the Magnetodisc Field on Plasma Injection Signatures at Saturn

SM33E-3264

P. Guio[1,2], N. Achilleos[1,2], C. Paranicas[3]

[1] Department of Physics and Astronomy, University College London (UCL), UK; [2] Centre for Planetary Science, UCL/Birkbeck;

[3] John Hopkins University Applied Physics Laboratory, USA

Email contacts: p.guio@ucl.ac.uk, nicholas.achilleos@ucl.ac.uk, chris.paranicas@jhuapl.edu

Download poster from `http://www.ucl.ac.uk/~ucappgu`

Abstract

Studies of plasma injection signatures at the giant planets commonly interpret these events in terms of a longitudinally localised 'bundle' of hot plasma or a more radially-extended flow channel. In either picture, the hotter plasma moves radially inward toward the planet and gains energy. These structures also entrain energetic charged particles. These charged particles have important azimuthal secondary drifts, eventually removing them from the injection location at different, energy-dependent velocities, leading to the 'dispersed' signature in observed energy spectra. In this study, we revisit the modelling of azimuthal gradient and curvature drift rates for injected particles, using a magnetodisc field rather than the pure dipole which is often assumed. We comment on the quantitative effect of the magnetodisc field on the energy dispersion of older injection events at Saturn where simultaneous multiple energy bands are observed in Cassini LEMMS proton data.

Energetic Charged Particle Injection Events

- Observed in the inner magnetosphere of gas giant planets since the beginning of the in-situ exploration of these worlds (*Mitchell et al.*, 2015).
- Thought to be the result of *flux-tube interchange* driven by strong centrifugal force associated with the rapid rotation of these planets (*Mauk et al.*, 1999).
- Characterised by an inward flow channel of longitudinally confined hot plasma, while ambient plasma in adjacent regions moves slower outward.
- Inward motion of hot plasma is accompanied by *azimuthal dispersion* due to energy- and species-dependent *gradient–curvature drifts* (left panel Fig. 1).

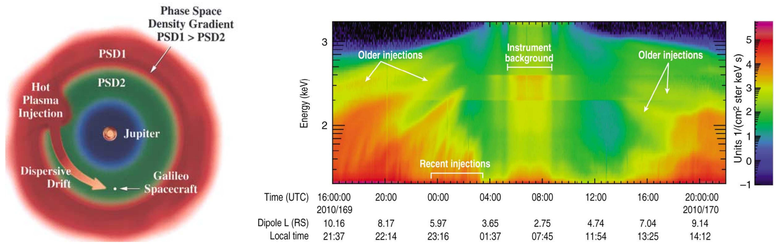

Figure 1. Left panel: simple concept to reproduce energy-time dispersed signatures of energetic particle injections at Jupiter (*Mauk et al.*, 2005, Fig. 3). Right panel: energy-time spectrogram of electron intensity from Cassini LEMMS instrument (*Paranicas et al.*, 2010, Fig. 1).

- Injections characterised as *recent* and *older*, with different signature (right panel Fig. 1).
- Focus on *very old* injections with *simultaneous multiple* energy bands (Fig. 2), interpreted as particles gradient-curvature drifted *a number of times* around the planet in *co-rotating* frame.

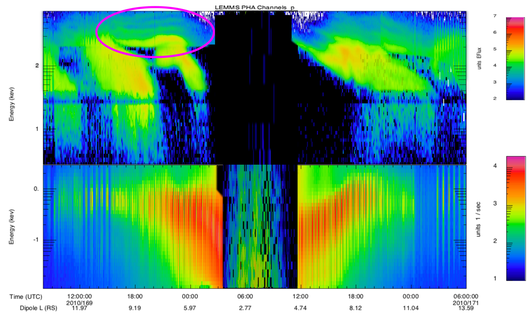

Figure 2. Energy-time spectrogram of proton intensity from Cassini LEMMS/PHA and CAPS instruments on 19 June 2010 with very old injection between 15:00–23:00 UTC (circled in magenta).

Magnetic Field Gradient and Curvature Azimuthal Drift

In the *guiding centre approximation*, the *bounce-averaged* azimuthal drift angular frequency Ω_d can be expressed as (*Thomsen and van Allen*, 1980; *Guio et al.*, 2019):

$$\Omega_d(E, R_{\rm eq}, \alpha_{\rm eq}) = \frac{3}{qB_{\rm P}R_{\rm P}^2} E \frac{E+2mc^2}{E+mc^2} R_{\rm eq} \frac{\Gamma(R_{\rm eq}, \alpha_{\rm eq})}{\Phi(R_{\rm eq}, \alpha_{\rm eq})}, \qquad (1)$$

where m, q and E are respectively the particle's mass, charge and kinetic energy, $R_{\rm eq}$ and $\alpha_{\rm eq}$ are the particle distance and pitch angle at the equator. The dimensionless integrals $\Gamma = \Gamma_c + \Gamma_g$, of the gradient and curvature contributions to azimuthal drift during a bounce period characterised by Φ are defined in (*Guio et al.*, 2019).

Azimuthal Drift for Kronian Magnetodisc

The UCL Magnetodisc model (*Achilleos et al.*, 2010) uses the formalism developed in *Caudal* (1986) to compute axisymmetric models of the rotating Kronian/Jovian plasmadisc in which magnetic, centrifugal and plasma pressure forces are in equilibrium.
We use the output of the model for a *standard* Kronian disc configuration with magnetopause located at $R_{\rm mp} = 25\,{\rm R_S}$ and with hot ion population index $K_h = 2 \cdot 10^6\,{\rm Pa\ m\ T^{-1}}$.

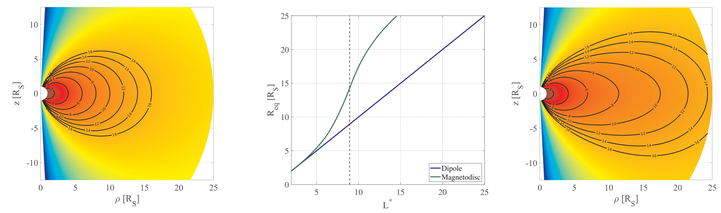

Figure 3. Left and right panels: Kronian dipole and magnetodisc fields. Middle panel: $R_{\rm eq}$ as function of the equivalent dipole L^*.

In Fig. 3, $R_{\rm eq}$ of both magnetodisc and dipole field lines is shown as a function of the parameter L^* – defined as $L^* = R_{\rm eq}$ for the dipole. For the magnetodisc, L^* denotes the equatorial distance of a dipole field line which emanates from the *same ionospheric footpoint*.
We calculated numerically the dimensionless integral Γ/Φ in Eq. (1) for $R_{\rm eq} = 2$–$12\,{\rm R_S}$ and $\alpha_{\rm eq} = 16$–$72\,^\circ$, seen in Fig. 4, and computed an estimate of Γ/Φ to a bi-variate polynomial in $R_{\rm eq}$ and $\sin\alpha_{\rm eq}$ to account for the equatorial stretching of the magnetodisc field lines:

$$\Omega_d(E, R_{\rm eq}, \alpha_{\rm eq}) \sim \frac{3}{qB_{\rm S}R_{\rm S}^2} E \frac{E+2mc^2}{E+mc^2} R_{\rm eq} \left(p_{00} + p_{01}\sin\alpha_{\rm eq} + p_{11} R_{\rm eq}\sin\alpha_{\rm eq}\right). \qquad (2)$$

Best fit for the coefficients p_{ij}'s of the monomials in Eq. (2) together with their uncertainties, for the dipole and magnetodisc fields in Fig. 3, are given in the table below with the coefficient of multiple determination R^2, and the root-mean-squared residual RMSE. The fit raw residuals for the magnetodisc $\Gamma^{\rm m}/\Phi^{\rm m}$ is also seen in Fig. 4. Note the non negligible value of p_{11} that characterises the magnetodisc.

	p_{00}	p_{01}	p_{11}	R^2[%]	RMSE
$\Gamma^{\rm d}/\Phi^{\rm d}$	$0.35\ (1{\cdot}10^{-5})$	$0.15\ (1{\cdot}10^{-5})$	–	100.0	0.00045
$\Gamma^{\rm m}/\Phi^{\rm m}$	$0.41\ (1{\cdot}10^{-3})$	$0.08\ (2{\cdot}10^{-3})$	$0.02\ (1{\cdot}10^{-4})$	58.6	0.047

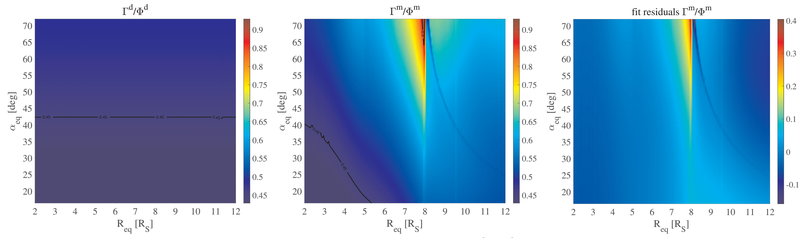

Figure 4. Left to right panels: numerically computed $\Gamma^{\rm d}/\Phi^{\rm d}$ and $\Gamma^{\rm m}/\Phi^{\rm m}$, and $\Gamma^{\rm m}/\Phi^{\rm m}$ fit residuals to the polynomial approximation with coefficients p_{ij}'s given in the Table above.

Older Injection Modelling

- Assume azimuthal drift ϕ *only* from point of channel exit ('source') thus no radial motion.
- For particles with *same* $R_{\rm eq}$ *and* $\alpha_{\rm eq}$, Ω_d is *only* a function of kinetic energy, thus the time delay ΔT from the injection source, located $\Delta\phi$ away is $\Delta T = \Delta\phi/\Omega_d(E)$.
- Consider two particles with energy E_0 and E_1 ($E_1{>}E_0$). Particle with E_1 will catch up particle with E_0 when $\Delta\phi/\Omega_d(E_0) = (\Delta\phi + 2\pi)/\Omega_d(E_1)$.
- Generalise to a particle with energy $E_n{>}E_0$ catching up particle with E_0 after n times with around the planet in the same time delay ΔT yields:

$$\Delta T = \frac{\Delta\phi}{\Omega_d(E_0)} = \frac{\Delta\phi + 2\pi n}{\Omega_d(E_n)}. \qquad (3)$$

- At *fixed* $R_{\rm eq}$ and $\alpha_{\rm eq}$, the ratio $\Omega_d(E_0)/\Omega_d(E_n)$ depends *only* on E_0 and E_n, as seen in Eq. (1).
- For *a given* $\Delta\phi$, *only* one set of energies $\{E_0, \cdots, E_n\}$ satisfies Eq. (3), see left panel in Fig. 5.
- The time delay ΔT from the source event is always shorter for the magnetodisc by up to $\sim$20%, see right panel in Fig. 5.

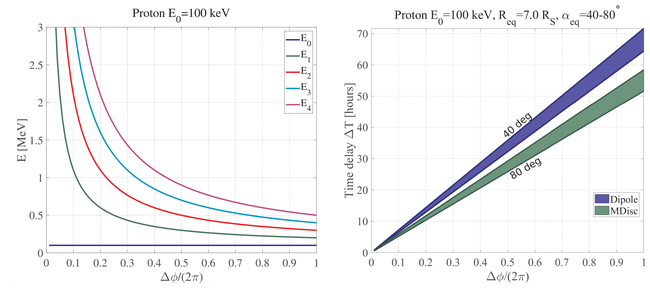

Figure 5. Solutions E_n of Eq. (3) as function of $\Delta\phi$ for $\rm H^+$ with $E_0{=}100\,{\rm keV}$; and corresponding time delay $\Delta T{=}\Delta\phi/\Omega_d$ of dipole and magnetodisc for $R_{\rm eq}{=}7\,{\rm R_S}$ and $\alpha_{\rm eq}{=}40$–$80\,^\circ$.

Results

We apply this injection model for the event seen in Fig. 2 to estimate the best fit for the energies E_n and the corresponding time delay from the source (Fig. 6).

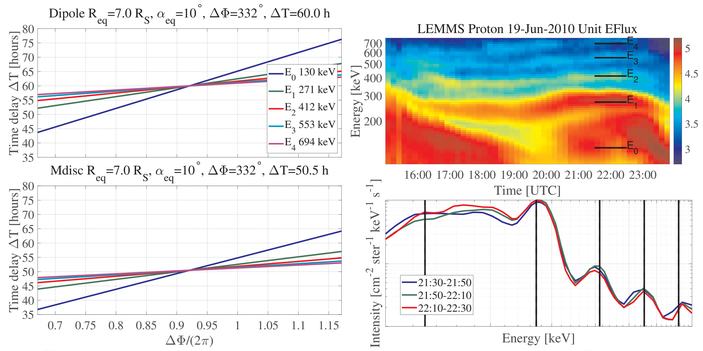

Figure 6. Fit of the multiple energy bands seen in the injection event in Fig. 2.

Conclusion

The banding structure of older injection has been interpreted as due to particles that have gradient-curvature drifted in the co-rotating frame a different number of times around the planet before detection.
A proper assessment of the gradient curvature drift rate is needed. We have developed the formalism for this rate beyond the dipole approximation and have tested our modelling of older injection on Cassini LEMMS proton data.
The results show that the time delay with the magnetodisc is reduced by up to $\sim$20% compared to the dipole. Therefore, there are implications for the accuracy of estimated residence times of these types of drifting particles.

References

Achilleos, N., P. Guio, C. S. Arridge, N. Sergis, R. J. Wilson, M. F. Thomsen, and A. J. Coates, Influence of hot plasma pressure on the global structure of Saturn's magnetodisk, *Geophys. Res. Lett.*, *37*, L20,201, doi:10.1029/2010GL045159, 2010.

Caudal, G., A self-consistent model of Jupiter's magnetodisc including the effects of centrifugal force and pressure, *J. Geophys. Res.*, *91*, 4201–4221, 1986.

Guio, P., N. Staniland, N. A. Achilleos, and C. S. Arridge, Trapped particle motion in magnetodisc fields, in preparation, 2019.

Mauk, B. H., D. J. Williams, R. W. McEntire, K. K. Khurana, and J. G. Roederer, Storm-like dynamics of Jupiter's inner and middle magnetosphere, *J. Geophys. Res.*, *104*, 22,759–22,778, doi:10.1029/1999JA900097, 1999.

Mauk, B. H., J. Saur, D. G. Mitchell, E. C. Roelof, P. C. Brandt, T. P. Armstrong, D. C. Hamilton, S. M. Krimigis, N. Krupp, S. A. Livi, J. W. Manweiler, and C. P. Paranicas, Energetic particle injections in Saturn's magnetosphere, *Geophys. Res. Lett.*, *32*, L14S05, doi:10.1029/2005GL022485, 2005.

Mitchell, D. G., P. C. Brandt, J. F. Carbary, W. S. Kurth, S. M. Krimigis, C. Paranicas, N. Krupp, D. C. Hamilton, B. H. Mauk, G. B. Hospodarsky, M. K. Dougherty, and W. R. Pryor, Injection, Interchange, and Reconnection, in *Magnetotails in the Solar System*, *Washington DC American Geophysical Union Geophysical Monograph Series*, vol. 207, edited by A. Keiling, C. M. Jackman, and P. A. Delamere, pp. 327–343, doi:10.1002/9781118842324.ch19, 2015.

Paranicas, C., D. G. Mitchell, E. Roussos, P. Kollmann, N. Krupp, A. L. Müller, S. M. Krimigis, F. S. Turner, P. C. Brandt, A. M. Rymer, and R. E. Johnson, Transport of energetic electrons into Saturn's inner magnetosphere, *J. Geophys. Res.*, *115*, A09214, doi:10.1029/2010JA015853, 2010.

Thomsen, M. F., and J. A. van Allen, Motion of trapped electrons and protons in Saturn's inner magnetosphere, *J. Geophys. Res.*, *85*, 5831–5834, doi:10.1029/JA085iA11p05831, 1980.